Automated intraoperative calibration for prostate cancer brachytherapy

Thomas Kuiran Chen, Tamas Heffter, Andras Lasso, and Csaba Pinter
Queen's University, Kingston, Ontario K7L 3N6, Canada

Purang Abolmaesumi
The University of British Columbia, Vancouver, British Columbia V6T 1Z4, Canada

E. Clif Burdette
Acoustic MedSystems, Inc., Champaign, Illinois 61820-3979

Gabor Fichtinger
Queen's University, Kingston, Ontario K7L 3N6, Canada and Johns Hopkins University, Baltimore, Maryland 21218-2682

(Received 18 July 2011; revised 2 September 2011; accepted for publication 23 September 2011; published 31 October 2011)

Purpose: Prostate cancer brachytherapy relies on an accurate spatial registration between the implant needles and the TRUS image, called "calibration". The authors propose a new device and a fast, automatic method to calibrate the brachytherapy system in the operating room, with instant error feedback.
Methods: A device was CAD-designed and precision-engineered, which mechanically couples a calibration phantom with an exact replica of the standard brachytherapy template. From real-time TRUS images acquired from the calibration device and processed by the calibration system, the coordinate transformation between the brachytherapy template and the TRUS images was computed automatically. The system instantly generated a report of the target reconstruction accuracy based on the current calibration outcome.
Results: Four types of validation tests were conducted. First, 50 independent, real-time calibration trials yielded an average of 0.57 ± 0.13 mm line reconstruction error (LRE) relative to ground truth. Second, the averaged LRE was 0.37 ± 0.25 mm relative to ground truth in tests with six different commercial TRUS scanners operating at similar imaging settings. Furthermore, testing with five different commercial stepper systems yielded an average of 0.29 ± 0.16 mm LRE relative to ground truth. Finally, the system achieved an average of 0.56 ± 0.27 mm target registration error (TRE) relative to ground truth in needle insertion tests through the template in a water tank.
Conclusions: The proposed automatic, intraoperative calibration system for prostate cancer brachytherapy has achieved high accuracy, precision, and robustness. [DOI: 10.1118/1.3651690]

Key words: brachytherapy, prostate cancer, TRUS, intraoperative ultrasound calibration

I. INTRODUCTION

I.A. Clinical background and significance

Prostate cancer is the second most frequently diagnosed cancer and the sixth leading cause of cancer death in men.[1] Brachytherapy has emerged as a definitive treatment for early stage prostate cancer. The procedure entails permanent implantation of small radioactive isotope capsules (seeds) into the prostate to kill the cancer with radiation.[2]

Prostate brachytherapy is delivered with real-time transrectal ultrasound (TRUS) image guidance (Fig. 1). Typically, the probe is translated and rotated by a mechanical stepper in the rectum with its displacement and rotation angle tracked by encoders on the stepper. Individual TRUS images of prostate contours are then compounded into a volume based on which an implant plan can be created and radiation dose calculated. Finally, under real-time, intraoperative TRUS image guidance, the actual implants are delivered transperineally by needles inserted through a template that contains a rectilinear grid of guide holes. Success of this treatment depends on an accurate plan of radiation dosimetry and a precise delivery of the implant.

The intrinsic accuracy of a brachytherapy system is solely determined by a unique procedure called "calibration", where a spatial registration between the coordinate systems of the TRUS and the template must be established prior to the implant procedure. Inaccurate system calibration causes faulty needle and radiation source placement, which may directly contribute to dosimetry errors, toxicity, and treatment morbidity.[2–5]

I.B. Current brachytherapy calibration in practice

In current practice, brachytherapy system calibration is a laborious, three-stage process.

Stage 1: An operator (typically a medical physicist) ascertains whether the TRUS image truthfully represents the size and shape of scanned objects and whether a series of individual images can be correctly stacked in space to reconstruct an accurate TRUS volume. For these purposes, artificial objects (phantoms) are employed with known geometry suspended in tissue-mimicking gel (to match the speed of sound in tissue).[6] Phantoms are made commercially for these

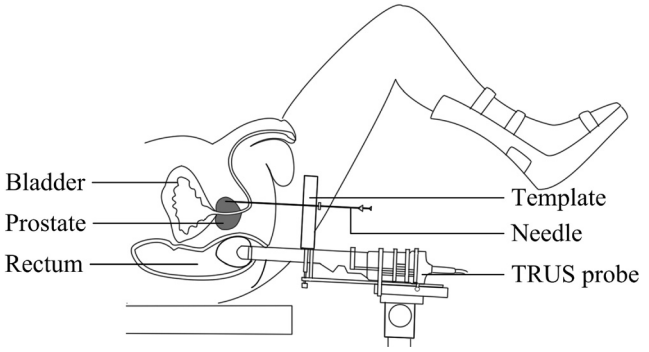

FIG. 1. TRUS-guided prostate-cancer brachytherapy: needles are inserted into the prostate through a template into a patient in the lithotomy position.

tasks; e.g., the industry-standard Brachytherapy Phantom CIRS 045 manufactured by Supertech, Elkhart, IN. (U.S. patent #5196343). The operator scans the phantom, measures the distance, size, shape, and volume of the visible 2D and 3D features in the TRUS images, and then compares them to the known geometric specifications provided by the phantom manufacturer. Such measurements are conducted manually using rulers and calipers, either on the display of the ultrasound scanner, or on the printed TRUS images.

Stage 2: The operator calculates the relative spatial transformation between the coordinate frame of the TRUS images and the coordinate frame of the template.[7] In the usual workflow, the operator mounts the template and the TRUS probe on a stand, dips the probe in a water tank, inserts needles through the template into the tank under TRUS imaging, marks the needle tips in the images, and calculates the transformation between the TRUS and template coordinate frames. For three needles a simple mathematical formula is available.

Stage 3: For some TRUS scanners that offer the ability to superimpose a square grid of coordinates on the real-time image, the overlaid grid lines must be aligned with the grids on the template. This is typically done by using eyesight and manually adjusting the scanner's setup. The user dips needles through the template into a water tank and then turns the knobs on the TRUS scanner until the grid lines appear to coincide with the artifacts created by the needles.[8]

There are a number of technical elements in the calibration workflow that can lead to substantial bias and error in the final result:

- The needles may be bent, therefore the segmented tip positions do not truthfully correspond to the physical locations of the template holes, which leads to erroneous template-TRUS registration;
- The needle tip may be inaccurately segmented, especially when beveled implant needles are used;
- The coordinates of the needle holes may be erroneously recorded;
- The depth of the needle may be erroneously measured and recorded;
- The number of needles used may be inappropriate; typically, too few needles are used;
- The distribution of needle positions may be inappropriate, introducing bias if needle tips do not properly surround the location of the prostate;
- The speed of sound in water is different from the speed of sound in human tissue, which can result in significant distance measurement errors in the TRUS image.

Overall, the procedure is laborious, more qualitative than quantitative, and involves a great deal of eyeballing and subjective judgments by the operator.

Furthermore, the calibration is performed only periodically (primarily due to the inefficiency of the procedure), mostly outside the operating room, with the assumption that calibration parameters remain valid over time. In reality, however, calibration parameters may change during storage, transportation and setup of the equipment.

Perhaps most critically, the system calibration errors are difficult to detect during the procedure so the brachytherapist has no assurance whether the system is functioning correctly in the operating room. There is no validation mechanism in the current procedure to verify and ascertain the calibration accuracy in the operating room.

Finally, brachytherapy calibration, with its current practice, is a major recurring cost for care facilities, consuming manpower, time and money. One must book a calibration room, decommit the TRUS unit from clinical use, transport the equipment, prepare supplies (needles, water tank, etc.), set up the system, collect and process data, and log, analyze and document the results, dispose all used supplies, pack away the brachytherapy system, and return the TRUS scanner to the clinic. This workflow needs to be repeated from time to time.

I.C. Ultrasound calibration technologies in the literature

TRUS calibration is implicitly present in the brachytherapy procedure, which may be the reason that so few publications have been dedicated to this problem.[7,8] In a greater context of tracked freehand ultrasound (US) imaging, however, many US calibration technologies have been explored. Tracking is typically achieved by rigidly affixing the probe with a localizer traced by a position sensing system.[9] Calibration is typically conducted by scanning an artificial object with known geometries, referred to as the "phantom". Widely used calibration phantoms include the single-point or cross-wire phantoms,[10–12] the three-wire phantom,[11] the single-wall and Cambridge phantoms,[11] the Hopkins phantom,[13] the Z-fiducial or N-wire phantoms,[14–19] and the Sandwich phantom.[20] Regardless of the various phantom designs in the literature, the fundamental idea behind this process remains the same: to identify features in both the acquired images and in the physical phantom space (which is known to us by construction). With both the position of the transducer and the phantom tracked by a localization system, an equation can then be built to convert between these two coordinate systems. An exception to this were the recently proposed phantomless (also referred to as *self-calibrating*) calibration techniques,[21,22] where images from actual patient

were used instead of a specific calibration phantom. A recent, comprehensive overview of US calibration techniques can be found in Mercier *et al.*[23]

To solve for the calibration parameters, a general approach is to employ least-mean squares to minimize the distance between the features of interest in the image space and the phantom space. If an exact correspondence of the features between the two spaces can be established, a *closed-form* solution is generally preferred[14–20]; if on the other hand, the precise location of features in the phantom space is unknown (which is the case for some phantom designs), then a method based on *iterative regression* must be used.[10–13]

Iterative approaches are, in general, less robust than closed-form solutions because of nonguaranteed convergence, potential trapping in local minima, and being sensitive to initial estimates.[26] Also, to achieve adequate accuracy, iterative methods typically need more input data and computational time than closed-form techniques. For instance, calibration with the Cambridge phantom[11] would require at least 550 images to achieve acceptable accuracy, as compared to around 6–30 images with a typical N-wire phantom.[14–18] On the other hand, closed-form solutions face the challenge to automatically and accurately extract point-targets from an ultrasound image and are therefore typically conducted manually, which is undesirable in the operating room. Though the majority of the point-based calibration technologies are manual and laborious, there have been successful attempts to automate segmentation of images acquired from N-wire phantoms.[15,18,19]

Finally, it is always desirable to have automatic, real-time feedback of calibration accuracy in the operating room. Boctor *et al.* were among the first to introduce a real-time *in-vivo* quality control mechanism that monitored the consistency in calibration parameters through frequent recalibration in the background.[22,27] However, their validation on the calibration results was based on precision and not accuracy. It is important to note that a measure of precision is quite different from that of accuracy[23]: precision defines the repeatability and consistency of the system, while accuracy evaluates how much the output is away from a known "ground truth" (typically measured independently). Not relying on a ground truth, a high precision (a low variance in results) does not necessarily guarantee a high accuracy. For example, it is possible that a calibration system that achieves highly consistent results may include a systematic error that renders the system inaccurate.

I.D. Contributions of this work

In this work, we aim to remove the aforementioned problems by performing the conventional brachytherapy template calibration tasks (Stage 2 and Stage 3) at once. We have developed a fast, automated, pure-computation based, intraoperative calibration (iCAL) technology for prostate cancer brachytherapy, intended to be used in the operating room when the patient is being prepared for surgery. Our method eradicates the current practice of preoperatively performed, labor-intensive and subjective calibration processes. The new calibration technology may simultaneously reduce treatment costs, increase safety and improve on the accuracy of all prostate cancer brachytherapy systems.

The remainder of this paper is organized as follows. First, an overview of the iCAL system is given. Then, the design and specifications of the calibration phantom are presented. Then, TRUS image acquisition and position tracking are discussed, together with the synchronization requirement (temporal calibration) between these two processes. Further, the automatic segmentation algorithm is explored step by step. We then reveal the details of our closed-form calibration solution, and illustrate iCAL's real-time accuracy evaluation mechanism. Finally, we present the experimental setup and validation results obtained with multiple, commercially available TRUS scanners and brachytherapy stepper systems, followed by discussions and conclusions in the end.

II. MATERIALS AND METHODS

II.A. iCAL system design and workflow

The design of iCAL entails a new device and an automated, computational method to calibrate the brachytherapy systems, intended to be performed in the operating room. The essence of this invention is a mechanical coupling of a precision-made calibration phantom and a geometric replica of a standard brachytherapy template, which effectively combines the iCAL phantom with the brachytherapy stepper system as one member (Fig. 2). This unibody design shares some similarity with the design of a phantom developed by Ng *et al.* for registration of TRUS and cone-beam CT.[24]

The fixture is mounted over the TRUS probe on the stepper, using the standard mounting posts and holes provided for the template. The TRUS probe makes contact with a rubber-membrane window on the posterior (bottom) side of the phantom, where the probe can be translated and/or rotated to acquire TRUS images from the interior of the phantom. The details of the phantom design are given in Sec. II B.

Figure 3 shows the workflow of iCAL consisting of five consecutive stages.

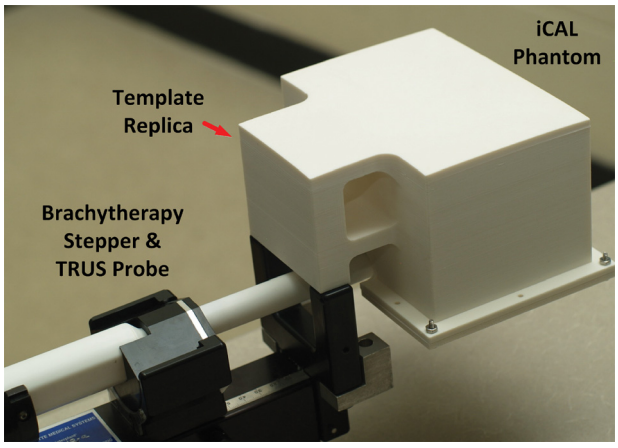

FIG. 2. Design of the iCAL system: calibration phantom mounted on a standard brachytherapy stepper.

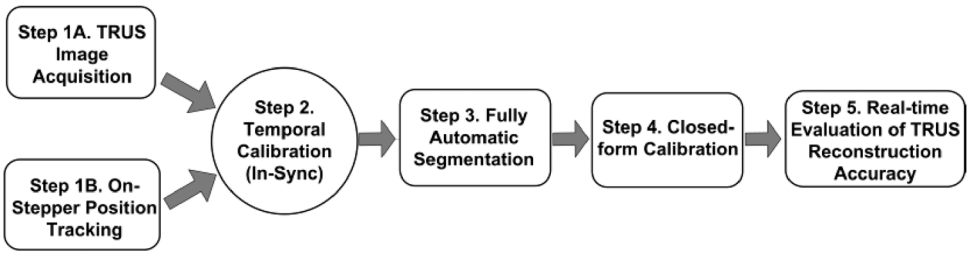

FIG. 3. Workflow of the iCAL brachytherapy calibration procedure.

1. Serving as input, TRUS images are continuously acquired from the iCAL phantom (Step 1A). The motion (translation and rotation) of the TRUS probe is tracked by the brachytherapy stepper (Step 1B).
2. A temporal calibration process is performed to synchronize the individual TRUS image frames with their respective positions (Step 2).
3. The TRUS images of the iCAL phantom are automatically segmented to extract the pixel locations of the phantom geometry (Step 3).
4. The pixel locations of the segmented phantom features, together with their corresponding physical coordinates collected in the phantom space, are fed to a closed-form formula to calculate the calibration parameters (Step 4).
5. Measured by a reconstruction error against a known ground truth, the accuracy of the calibration result is fed back to the control loop to determine whether or not it is satisfactory. The reconstruction accuracy is updated, monitored and displayed in real time. Once the process converges or the reconstruction error reaches an acceptable level, the procedure is terminated and the final calibration outcomes exported (Step 5).

Compared to the conventional, manual brachytherapy calibration (Stages 2 and 3), iCAL accomplishes all the required tasks in one automated loop. First, the calibration outcome from iCAL contains the homogenous spatial transformation parameters that register the TRUS image plane to the template. This accomplishes Stage 2 of the conventional calibration.

Second, as a byproduct of the calibration results, iCAL overlays the location of the template grid onto the transverse TRUS image, and in real time updates and displays a virtual grid through an interactive graphics interface to the user whenever the probe is being translated and/or rotated. This accomplishes Stage 3 of the conventional calibration.

From a software-architecture point of view, iCAL was designed and developed using a multiple-component-based object-oriented methodology.[25] In addition to the unique calibration phantom design, iCAL encompasses five essential system components: *TRUS image acquisition and tracking*, *temporal calibration*, *automatic segmentation*, *closed-form calibration*, and *real-time reconstruction accuracy feedback*. A number of open-source software libraries were employed, including the Visualization Toolkit (VTK), QT and Vision Numerics Library (VNL).

II.B. iCAL phantom design

The iCAL calibration phantom mechanically combines a precision-engineered, N-wire (Z-fiducial) calibration phantom and an exact, exterior replica of the brachytherapy template into one member, as part of the phantom geometry.

For geometric precision and structural integrity, the iCAL phantom was first designed in the Solid Edge CAD software [Fig. 4(a)]. The CAD model was then exported to a Dimension 1200es 3D Printer (Stratasys, Inc., Eden Prairie, MN) to manufacture the parts using a production-grade, high-density, high-strength, and liquid-proof thermoplastic. There are three individual parts designed to complete the phantom assembly [Fig. 4(b)]: a container box, an inner N-wire mount, and a sealing cover.

The container box embeds the exterior replica of the template and was measured to be $156 \times 96 \times 92$ mm in size [Fig. 4(b)]. In our prototype design, to approximate the speed of sound in tissue (1540 m/s), the container box was filled with distilled water heated to a temperature of around 37 °C, at which sound travels at approximately 1570 m/s.[28] In the final product, the box will be sealed with acoustic coupling medium to exactly match the speed of sound in tissue.

The inner N-wire mount is replaceable and fits snugly in the container box, with dimensions of $146 \times 80 \times 62$ mm [Fig. 4(c)]. It consists of a front and a back plate connected by two side walls, forming a simple open-ended box. There are holes on both the front and back plate to mount the N-wires. The N-wires are made of nylon line at 0.4 mm in diameter, a size comparable to the TRUS wavelength used for prostate imaging (ranging typically from 0.2 to 0.5 mm) which would optimize the image appearance of the wires.[19] The location of the N-wires encompasses the targeted area of the prostate in a clinical setup, thus maximizing the calibration accuracy.

The sealing cover contains a rubber window for TRUS imaging [Fig. 4(d)]. A 0.8 mm thick, natural rubber membrane (manufactured by McMaster-Carr, Inc., Robbinsville, NJ) forms the imaging window on the posterior (bottom) side of the phantom. Natural rubber has an acoustic impedance (1.81 Mrayls) that is similar to that of water (1.48 Mrayls), allowing sound transmission in and out of the container with only small attenuation.

Finally, the embedded replica is made from the brachytherapy template model D1-1784RA (Burdette Medical Systems, Inc., Champaign, IL) that measures $81.0 \times 71.1 \times 19.1$ mm

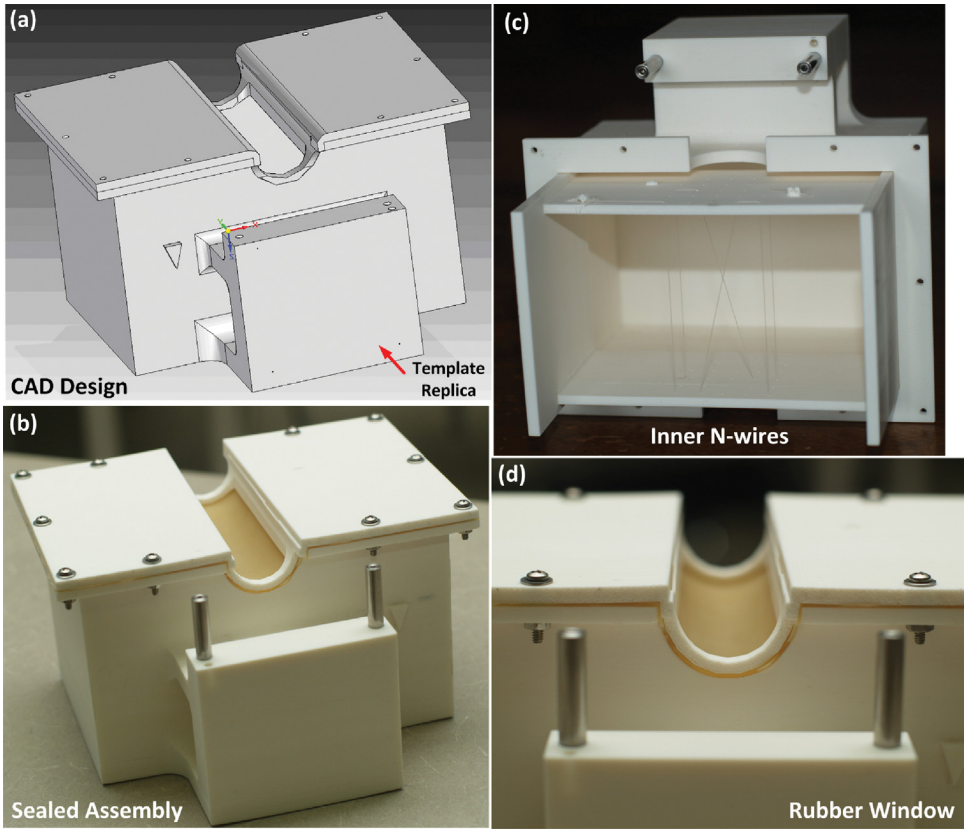

FIG. 4. iCAL phantom: CAD design, inner N-wires, complete assembly, and rubber seal.

in dimensions and has a matrix of 13×13 holes at 5-mm spacing vertically and horizontally.

There are two immediate benefits of this unibody design to mechanically couple the iCAL phantom to the template replica. First, it preempts the sterilization issues of the phantom, because it would be otherwise impractical to attach the phantom to the template which needs to be sterilized in the operating room. Second, the precision-engineering design and prototyping ensure a very high accuracy and precision in localizing the phantom geometry during the calibration process.

II.C. TRUS image acquisition, tracking, and temporal calibration

II.C.1. TRUS image acquisition

iCAL is equipped with two common types of TRUS image acquisition interfaces: an analogue and a digital data acquisition.

II.C.1.a. Analogue data acquisition. The TRUS images are transferred from the analogue data output (e.g., S-Video or Composite port) of the TRUS scanner to an ImageSource DFG/USB2-LT USB framegrabber (Imaging Source, LLC., Charlotte, NC) installed in the host computer at 30 frames per second (fps). The major benefit of using the analogue data output lies in the fact that it is the most common interface available on a standard TRUS machine, therefore provides the best hardware compatibility for iCAL to work with virtually any commercially available TRUS scanners currently in the market. The major downside however, is the relatively lower image quality compared to the digital format. Because the ultrasound machine processes and stores all scan-converted image data digitally in its internal memory, a digital-to-analog (D/A) conversion of the data needs to be performed when outputting the signals to the analog video port, which is then converted back to digital by the USB video-capturing device on the host computer. This double conversion results in a degradation in image quality of the original, digital image.[28] We have tested the analogue data acquisition with iCAL on five commercially available TRUS scanners:

- Leopard 2001 (BK-Medical Systems, Inc., Peabody, MA,
- Sonix MDP 4.0 Analogue Output (Ultrasonix Medical Corp., Burnaby, BC, Canada),
- Sonix TOUCH Analogue Output (Ultrasonix Medical Corp., Burnaby, BC, Canada),
- VLCUS (Carolina medical Systems, Inc.,),
- Terason 2000 (Teratech Corp., Burlington, MA).

II.C.1.b. Digital data acquisition. For better imaging quality, higher data acquisition speed and research purposes, some TRUS scanners on the market now offer a digital interface to acquire images directly from the internal image memory of the ultrasound machine. In iCAL, we have also developed a digital data acquisition based on the OPENSonix platform from Ultrasonix Medical Corp., Burnaby, BC, Canada. We have tested the digital data acquisition with iCAL on Ultrasonix SonixMDP and SonixTOUCH scanners.

II.C.2. Stepper position tracking

While the TRUS images are being continuously acquired from the iCAL phantom, the motion of the TRUS probe is simultaneously tracked by the brachytherapy stepper. Typically, there are two separate, optical encoders to independently track the motion of the TRUS probe in real time: a translation encoder that reads the displacement of the probe along the *Z*-axis, and a rotation encoder that reads the rotation of the probe transversely. This position data is then retrieved back to the host computer via a serial-port connection to be associated with the image data. We have tested iCAL with two types of brachytherapy stepper systems that are currently commercially available on the market:

- Target Guide Stepper (Burdette Medical Systems, Inc., Champaign, IL),
- Accuseed DS300 Stepper (Computerized Medical Systems, Inc., Saint Louis, MO).

II.C.3. Temporal calibration

Since the images and the tracked probe positions are generated by separate hardware (the TRUS scanner and the stepper tracking system), proper synchronization between the two must be established to correctly associate each acquired TRUS image with its corresponding positional data. This process is commonly referred to as the "temporal calibration".[23]

When a TRUS image is acquired and its corresponding stepper position recorded, both data can be time-stamped. However, this time-stamping process itself introduces some delay, because of the difference in processing speed between the ultrasound machine and the stepper system, as well as the necessary time required for data transfer (from the ultrasound machine and the stepper system to the host computer). The goal of a temporal calibration is to determine this delay ("latency"). Temporal calibration is typically conducted by introducing some form of abrupt change in the motion of the ultrasound transducer that would also result in a traceable difference in the ultrasound image.[29–35] The basic idea is to identify and match this difference in both the positional data and in the ultrasound image, based on which a latency between the tracking and image acquisition is then computed.

For iCAL, we have developed a fast and automated temporal-calibration technique by repeatedly and rapidly pausing and translating the TRUS probe on the stepper every two seconds while imaging the iCAL phantom. Figure 5 shows an example of the results of the temporal calibration in iCAL. The abrupt and repeated motion caused positional changes in both the TRUS image contents and the stepper readings, which were automatically detected and registered together to compute the temporal latency.

II.D. Automated segmentation

Demanding no human interference at all, we developed an algorithm to automatically segment images acquired from the iCAL calibration phantom. The typical cross-section view of a wire is a single small dot in the TRUS image, which is challenging for automatic segmentation for point-based calibration technologies.[23] A major difficulty is how to accurately and robustly recognize the point targets in the presence of speckle, which has similar image intensities and shapes. The basic idea was to utilize two unique geometric features of N-fiducials in the image to assist the segmentation: the three *collinear* dots that form an N-wire intersection with the TRUS image plane and the two nearly *parallel* lines that pass through these two layers of dots.

The segmentation algorithm contains four stages with various image processing techniques involved. First, dominant speckles are removed by a series of morphological operations. Pixels are then clustered to yield possible candidates of dots. Now we search for lines composed of three dots, and further narrow the search space to a pair of two such lines close to being parallel. This four-stage algorithm works effectively with noisy input data with speckles, reflections and other typical ultrasound artifacts. For more technical details of the automated segmentation algorithm, please refer to our prior work.[36]

II.E. The closed-form calibration method

The general idea behind ultrasound probe calibration is to identify features in both the acquired images and in the physical phantom space (which is known to us by construction.)[23]

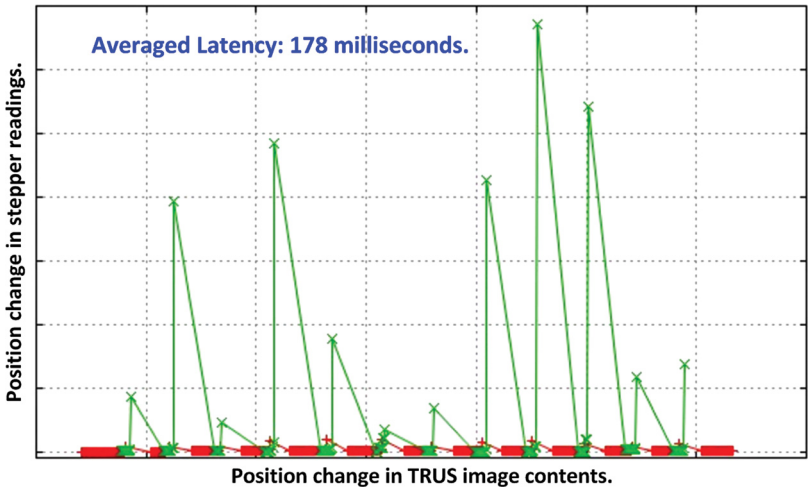

FIG. 5. An example of the automated temporal calibration in iCAL.

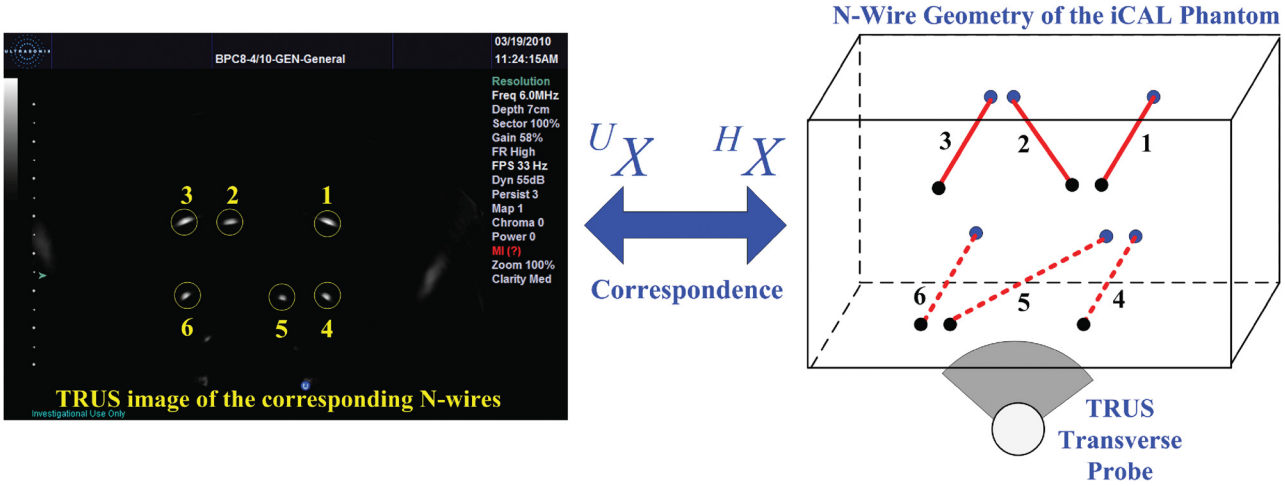

FIG. 6. The unique N-wire geometry of the iCAL calibration phantom.

With both the position of the transducer and the phantom tracked by a localization system, an equation can then be built to transform between these two coordinate systems.

Figure 6 shows the N-wire geometry of the iCAL calibration phantom, from which we can solve for the calibration parameters in a single closed-form equation. In the general case, let ^{A}X and ^{B}X denote 3D positions X expressed in coordinate frames A and B, respectively. $^{B}_{A}T$ then represents a homogeneous transformation[37] that maps ^{A}X to ^{B}X, as expressed by the generic equation:

$$^{B}X = {}^{B}_{A}T \cdot {}^{A}X. \tag{1}$$

In the present case, objective of the calibration is to determine $^{P}_{U}T$, the transformation that brings a position from the TRUS image frame (U) to the TRUS probe frame (P) through a series of 3D spatial frame transformations as depicted by Fig. 7. Note that $^{P}_{U}T$ is a 4×4 matrix that encodes 8 calibration parameters (3 rotation parameters, 2 scaling factors, and 3 translation parameters) in a single homogeneous transformation.[37]

To start, we first acquire a set of TRUS images from the iCAL calibration phantom. The intersection point of a wire and the TRUS image plane would display a gray-intensity dot in the image, which could be expressed in the TRUS image frame (U) and in the phantom frame (H) as ^{U}X and ^{H}X, respectively (Fig. 6):

$$^{U}X = ({}^{P}_{U}T)' \cdot {}^{P}_{S}T \cdot {}^{S}_{H}T \cdot {}^{H}X. \tag{2}$$

On the left side of Eq. (2), ^{U}X could be measured as the N-wire positions in the TRUS image frame. On the right side, $^{P}_{S}T$, the transformation from the stepper frame to the TRUS probe frame, was known from the stepper's position tracking of the probe. $^{S}_{H}T$, the transformation from the phantom frame to the stepper frame, was known by the iCAL phantom design that mechanically couples the phantom geometry with an exact replica of the template affixed onto the stepper. ^{H}X is the corresponding physical position of ^{U}X in the phantom frame and can be calculated using the similar-triangle geometry of the N-wires.[36] Finally, $^{P}_{U}T$ is the unknown calibration parameter for which we wish to solve.

Both ^{U}X and ^{H}X can be expressed as 4×1 column vectors in homogeneous format, i.e., $^{U}X = [{}^{U}x \quad {}^{U}y \quad 0 \quad 1]'$ and $^{H}X = [{}^{H}x \quad {}^{H}y \quad {}^{H}z \quad 1]'$. For a number of m such N-fiducials, we can construct ^{U}X and ^{H}X in matrices as:

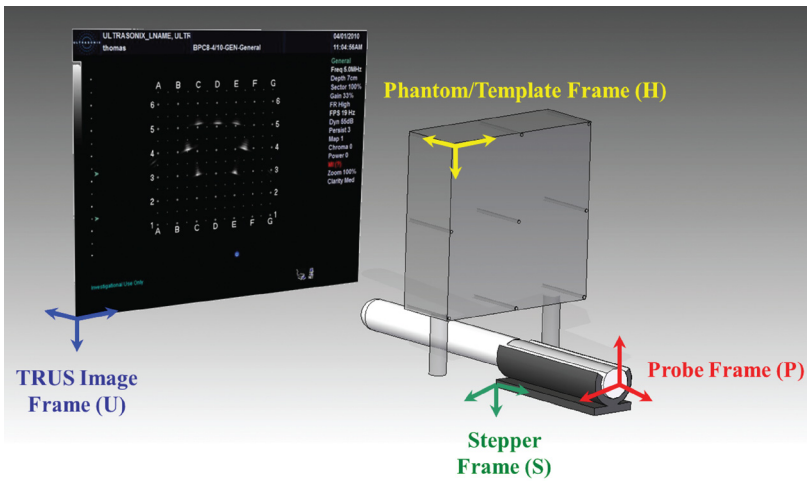

FIG. 7. Coordinate transformations from the template to the TRUS image.

$$
{}^{U}X = \begin{pmatrix} {}^{U}x_1 & {}^{U}x_2 & \cdots & {}^{U}x_m \\ {}^{U}y_1 & {}^{U}y_2 & \cdots & {}^{U}y_m \\ 0 & 0 & \cdots & 0 \\ 1 & 1 & \cdots & 1 \end{pmatrix}
$$

$$
{}^{H}X = \begin{pmatrix} {}^{H}x_1 & {}^{H}x_2 & \cdots & {}^{H}x_m \\ {}^{H}y_1 & {}^{H}y_2 & \cdots & {}^{H}y_m \\ {}^{H}z_1 & {}^{H}z_2 & \cdots & {}^{H}y_m \\ 1 & 1 & \cdots & 1 \end{pmatrix}. \tag{3}
$$

Note the difference in the 3rd rows between matrices of ${}^{U}X$ and ${}^{H}X$. Points in the TRUS image frame do not have a z-coordinate, so without losing generality we use all zeros for their 3rd components.

In all, what Eqs. (2) and (3) have established is an overdetermined system for ${}^{P}_{U}T$, which can be solved using a straightforward implementation of linear least squares. For N-wire-based calibration technologies, a minimum reported number of 120 data points (i.e., $m = 120$) are necessary for high-accuracy calibration.[14–16,36,40]

II.F. Real-time evaluation of calibration accuracy

Direct evaluation of calibration accuracy is typically challenging because of the lack of a reliable way to obtain the exact spatial relationship between the ultrasound image plane and the probe. A common work-around is to measure how closely a 3D reconstructed position is mapped from a ultrasound image (after applying the calibration parameters) to its true physical location (i.e., the ground truth). This type of accuracy measurement is generally referred to as a 3D reconstruction accuracy[23] and has been widely used in the ultrasound calibration literature.[12,36,38–40] The same principle can be extended to more complex structures, e.g., to scan a specially designed phantom[15] or, simpler, the calibration phantom itself.[14]

Similar to the approach proposed in Ref. 14, we employed the iCAL calibration phantom to test the calibration accuracy. We first scanned the iCAL phantom and reconstructed the cross-sections of four sets of parallel wires (#1, #3, #4, and #6 in Fig. 6) into the 3D world coordinate system using the computed calibration parameters. We then compared them, respectively, to their known physical locations (the gold standard) to compute a mean residual reconstruction error, defined as the line reconstruction error (LRE):

$$
\| LRE \| = \| {}^{H}X - {}^{H}_{S}T \cdot {}^{S}_{P}T \cdot {}^{P}_{U}T \cdot {}^{U}X \|, \tag{4}
$$

where ${}^{P}_{U}T$ is the calibration outcome to evaluate, ${}^{S}_{P}T$ is the transformation from the TRUS probe frame to the stepper frame given by the stepper's position readings, ${}^{H}_{S}T$ is the transformation from the stepper frame to the iCAL phantom frame that is known by the iCAL phantom geometry mechanically coupled to the stepper system, ${}^{U}X$ is the identified position of the wire in a TRUS image, and ${}^{H}X$ is the corresponding wire location known by the iCAL phantom design (as the ground truth).

There are several important facts to note about our calibration accuracy evaluation. First, LRE is an absolute *Euclidean* distance between a reconstructed point and the respective wire (i.e., a point-line distance) in space, so it remains invariant to frame transformations, and has units of millimeters.

Second, iCAL performs this error measurement in real time by automatically extracting the wire positions and reconstructing them in the physical phantom space using the computed calibration parameters.

Further, because the same phantom geometry is utilized for both calibration and accuracy evaluation, we separate the data used for LRE calculation from those used for calibration to avoid a systematic bias in the error evaluation toward the calibration results.

Finally, one significant advantage of this automatic error retrieval is that the process can be performed quickly and efficiently for an extensive data set collected from a variety of experimental conditions to thoroughly evaluate calibration quality. This has enabled us to quickly test iCAL

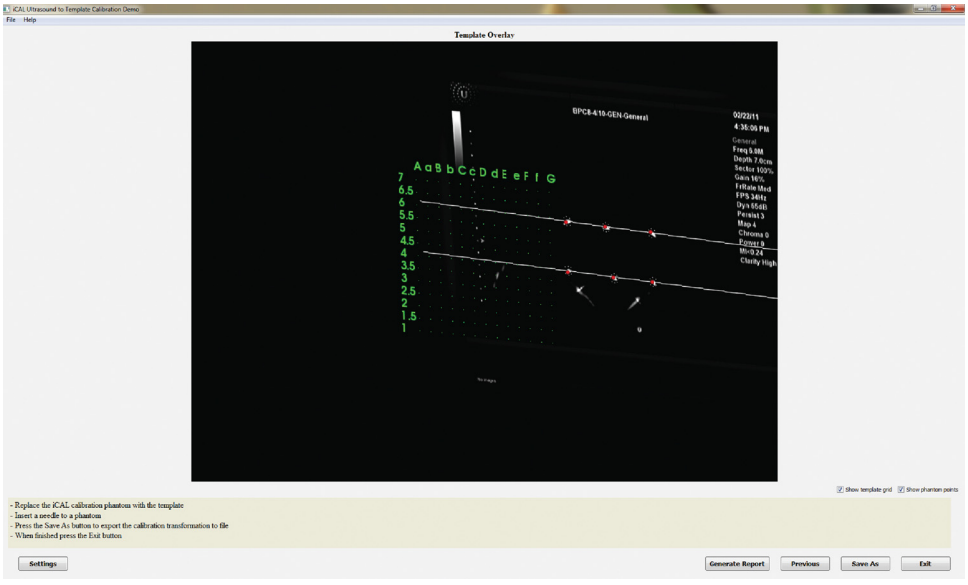

FIG. 8. The interactive graphics interface of iCAL showing the 3D overlay of the template grid to the TRUS image in real time.

through 50 independent calibration trials with the error computed in real time, which would not be possible for a conventional, manual brachytherapy calibration procedure.

II.G. Real-time overlay of the template grid on the TRUS images

Once the calibration parameters are computed, iCAL automatically registers (overlays) the location of the template grid onto the transverse TRUS image, and displays it to the users via an interactive 3D graphical user interface (Fig. 8). The user can rotate and enlarge the 3D scene to visually examine the spatial relationship between the TRUS image plane and the template grid. Note the matrix of green dots shown in Fig. 8 are the needle guiding holes on the front surface of the template.

iCAL also updates in real time the position change of the TRUS image and the template when the probe is being translated and/or rotated and when the template is being displaced by the user, respectively.

On newer TRUS scanners, such as the Sonix MDP or Sonix TOUCH (Ultrasonics, Inc., Burnaby, BC, Canada), the calibration parameters can also be set by iCAL through a manufacturer-provided application programming interface (API) to directly update the superimposed template grid on the display of the TRUS machine.

II.H. Experimental setup

To investigate the accuracy, precision, robustness, and speed of iCAL, we performed four types of independent tests:

- Experiments with 50 real-time independent calibration trials,
- Experiments with multiple different TRUS scanners,
- Experiments with multiple different brachytherapy stepper systems,
- Experiments with needle insertion to validate template-TRUS calibration.

II.H.1. Experiments with 50 real-time independent trials

This type of experiment was designed to validate the accuracy, reliability and speed of iCAL. In the experiment, the TRUS scanner used was a Sonix MDP 4.0 (Ultrasonics, Inc., Burnaby, BC, Canada) that operated at a central frequency of 6 MHz with an imaging depth of 7 cm. The TRUS image data was acquired digitally using the Ulterius SDK provided by the manufacturer. The stepper system used was a Target Guide Stepper (Burdette Medical Systems, Inc., Champaign, IL).

A total of 50 independent, real-time calibration trials were individually performed by iCAL, with the transducer inserted and attached to the stepper at all time. In each calibration experiment:

- A total of 300 live TRUS images were acquired from the iCAL phantom to compute the calibration parameters. For N-wire-based calibration technologies, a minimum reported number of 120 data points are necessary for high-accuracy calibration.[14–16,36,40] In the iCAL phantom design (Fig. 6) where two sets of N-wires are visible in a single TRUS image, the 300 images used for calibration would yield 600 data points, which is more than sufficient for the process to converge.
- Another 100 live TRUS images acquired from the iCAL phantom were used to compute the LRE [Eq. (4)] in order to evaluate the calibration accuracy. On each validation image, the positions of the wires #1, #3, #4, and #6 (Fig. 6) were automatically extracted and reconstructed in the 3D space using the calibration parameters. This yields 400 LRE measurements per experiment, from which a mean and standard deviation of the errors are calculated.
- This setup purposely prevents the same data from being used in both calibration and accuracy evaluation, which would create a biased validation.

Finally, the LREs from all 50 independent experiments were statistically analyzed.

II.H.2. Experiments with multiple different TRUS scanners

These experiments were designed to evaluate the robustness and compatibility of iCAL working with ultrasound machines of different data interfaces, types/sizes, ages, and manufacturers:

- Interfaces: analogue (S-video) and digital (proprietary API) data acquisition;
- Type/Size: full-size, portable and laptop size.
- Ages: some old and latest generations of TRUS machines were tested.
- Manufacturer: TRUS scanners are from four different manufacturers.

Table I lists the detailed setup for the experiments. In each experiment, 300 live TRUS images were acquired from the iCAL phantom to compute the calibration parameters, and then another 100 live TRUS images to compute the LRE. To limit the testing variable to the TRUS machines only, the same Target Guide Stepper (Burdette Medical Systems, Inc., Champaign, IL) was used through all the experiments.

II.H.3. Experiments with multiple different brachytherapy stepper systems

These experiments were designed to examine the robustness and compatibility of iCAL working with different brachytherapy stepper systems, offering varying position-tracking quality. The experiments included four different Target Guide Steppers and an Accuseed DS300 Stepper. In each experiment, 300 live TRUS images were acquired from the iCAL phantom to compute the calibration parameters, and then another 100 live TRUS images to compute the LRE. Table II gives the details of the tested stepper systems. To limit the testing variable to the stepper systems only, we used the digital data acquisition from Sonix TOUCH

TABLE I. Experimental setup with multiple TRUS scanners.[a]

TRUS Scanner	Manufacturer	Data Interface	Type	Age
Leopard 2001	BK-Medical Systems, Inc., Peabody, MA	S-video	Full	1980s
Sonix MDP 4.0	Ultrasonix Medical Corp., Burnaby, BC, Canada	S-video	Full	2000s
Sonix TOUCH (analogue)	Ultrasonix Medical Corp., Burnaby, BC, Canada	S-video	Full	2010s
Sonix TOUCH (digital)	Ultrasonix Medical Corp., Burnaby, BC, Canada	Ulterius Digital	Full	2010s
Terason 2000	Teratech Corp., Burlington, MA	S-video	Laptop	2000s
VLCUS	Carolina Medical Systems, Inc., NC	S-video	Portable	1990s

[a]Stepper used: Target Guide Stepper (Burdette Medical Systems).

(Ultrasonix Medical Corp., Burnaby, BC, Canada) for all the experiments.

II.H.4. Experiments with needle insertion to validate template-TRUS calibration

Finally, we validated the template-to-TRUS calibration/registration outcome by measuring a target registration error (TRE) with the water tank method.[7,8] Seven brachytherapy needles were inserted to the same depth through the template holes C3, C5, D5, E3, E5, b4, and e4 and scanned by TRUS in a water tank. The brachytherapy needles used in the tests are 18-gauge Mick TP Prostate Seeding Needles (Mick Radio-Nuclear Instruments, Inc., Bronx, NY), having a 1.270 ± 0.013 mm outer diameter. The TRUS image has a size of 640×480 pixels and a resolution of 0.2 mm/pixel (or 5 pixels per millimeter). The position of each needle tip in the TRUS image was manually segmented by an experienced human operator and then compared to the computed location by iCAL to obtain the respective TRE value.

III. RESULTS

III.A. Results of automated segmentation

We tested the automated segmentation algorithm with over 10,000 TRUS images acquired from the iCAL phantom. These images were taken at various displacements and rotation angles to cover every possible view of the N-wires. We then compared the segmentation outcomes with the ground-truth results identified by an experienced human operator. In all the images tested, there was no failure in identifying the N-wires and a careful inspection could not identify visible segmentation errors. Figure 9 shows an example of segmentation.

TABLE II. Experimental setup with multiple brachytherapy stepper systems.

Brachytherapy stepper	Manufacturer	Number of Units Tested
Target guide stepper	Burdette Medical Systems, Inc., Champaign, IL	4
Accuseed DS300 Stepper	Computerized Medical Systems, Inc., Saint Louis, MO	1

III.B. Results of experiments with 50 real-time independent trials

Table III shows the validation results for the 50 independent, real-time calibration trials performed by iCAL. LRE was computed as the "line-reconstruction error" or the "point-line distance", as defined in Eq. (4). The TRUS image has a size of 640×480 pixels and a resolution of 0.2 mm/pixel (or 5 pixels per millimeter).

Key findings include the following. First, all 50 calibration trials reached a sub-millimeter accuracy: the average LRE for all trials was 0.57 mm and the maximum error (the worst case scenario) was 0.91 mm. The clinical translation of this result into a brachytherapy procedure is that assuming there is no needle bending, the accuracy of needle insertion and seed placement based on the template-TRUS registration provided by iCAL would be 0.6 mm on average. In addition, this result is also consistent with the reconstruction accuracy reported for related ultrasound calibration literature using N-wires.[14–16,36,40]

Second, because the calculation of LRE is based on the ground-truth position of the wires #1, #3, #4, and #6 (Fig. 6) which, by the design of iCAL phantom, encompass the targeted area of the prostate in a clinical setup, the scope of the LRE provides a sound estimate of the accuracy in localizing anatomical targets in the prostate during a brachytherapy procedure.

Further, the standard deviation of the LRE was 0.13 mm, which suggests that iCAL also has an excellent precision in producing a consistent, and repeatable calibration. The very low variability in the calibration outcome is desirable for use in the operating room.

Finally, each of the 50 calibration trials converged in an average of 20 seconds (on an Intel Core 2 Duo Q6600 workstation at 2.4 GHz with 4 GB memory running Windows Server 2008R2 64-bit), sufficiently fast for use in the operating room.

III.C. Results of experiments with different TRUS scanners

Table IV shows the validation results of iCAL tested with different TRUS scanners. All experiments were conducted using the same Target Guide Stepper (Burdette Medical Systems, Inc., Champaign, IL.)

Our key observations and findings include the following. First, iCAL was able to consistently achieve a sub-millimeter, high calibration accuracy and precision across all the tested TRUS imaging platforms: the average LRE is 0.37 mm with a standard deviation of 0.25 mm.

There was no difference in iCAL's accuracy level between the digital data acquisition (Sonix TOUCH Ulterius API) and the analogue data acquisition from SVideo (the rest of the tested scanners), even though the digital platform

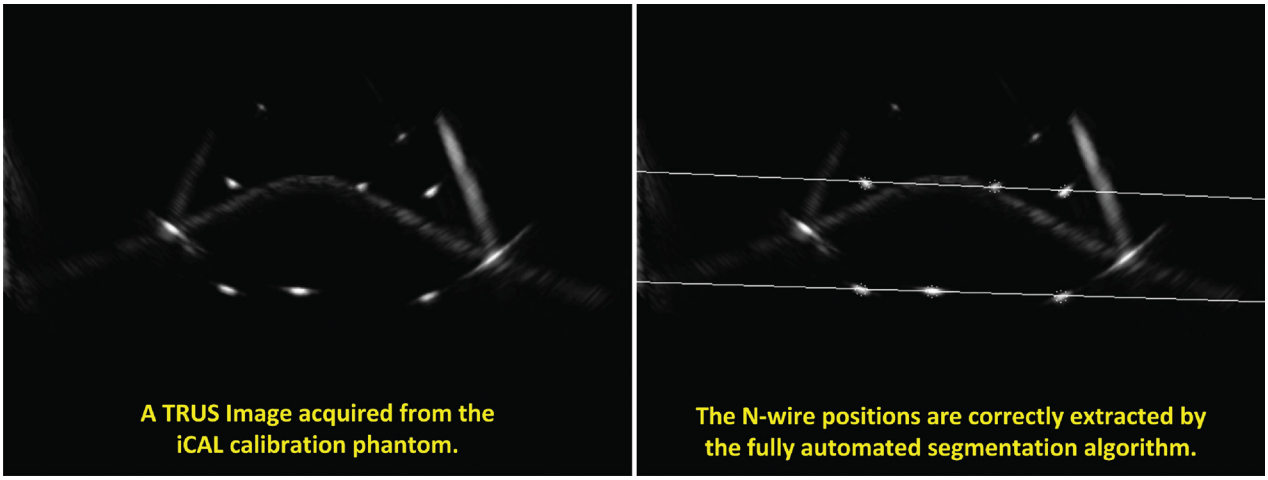

FIG. 9. Automatically segmented N-Wires from the TRUS image of the iCAL phantom.

offers better image quality (less noise) and finer per-pixel resolution than the analogue units. In our tests, the digital TRUS image has 0.2 mm/pixel resolution (or 5 pixels per millimeter) while the analogue image only has 0.26 mm/pixel resolution (or 3.8 pixels per millimeter). This suggests that iCAL does not demand high image quality and resolution to perform accurately, and would be compatible with the majority of TRUS machines currently on the market which are equipped with a standard analogue data output.

There was also no difference in iCAL's accuracy level between the latest TRUS machines (manufactured after 2000) and some of the older ones (manufactured in the 1990s). The newer TRUS scanners typically offer more polished hardware design and better signal transmission, retrieving and processing quality, which in turn results in overall better TRUS imaging quality than the older technologies. This result confirms the robustness of iCAL in dealing with varying TRUS hardware and imaging conditions.

Finally, iCAL achieved the same level of accuracy in different types of TRUS machines including standard full-size, portable and even laptop-size TRUS scanners. This suggests that iCAL does not require high-processing power from a typical full-scale TRUS system to function properly, which provides more flexibility and mobility in an intraoperative brachytherapy situation to work with small, portable TRUS devices if desired.

TABLE III. Validation results of iCAL for 50 independent, real-time calibration trials.

Number of Trials:[a] 50 (independent)	Line Reconstruction Error (LRE: mm)
Mean (μ)	0.57
Standard deviation (σ)	0.13
Minimum (best case)	0.26
Maximum (worst case)	0.91
Runtime[b]	20 s/trial

[a]With a Sonix MDP scanner and a target guide stepper.
[b]Intel Q6600 2.4GHz 4GB-RAM Windows Server 2008 64-bit.

III.D. Results of experiments with different brachytherapy steppers

Table V shows the validation results of iCAL tested with different brachytherapy stepper systems. In all experiments, the TRUS images were acquired from the Sonix TOUCH (Ultrasonix Medical Corp., Burnaby, BC, Canada) via the analogue SVideo data output using the USB framegrabber.

Key observations and findings include the following. iCAL was able to consistently achieve a sub-millimeter, high calibration accuracy and precision across all the tested brachytherapy stepper systems: LREs of all tests were below 0.5 mm with an average of 0.29 mm and a standard deviation of 0.16 mm. This suggests that iCAL is robust in working with different stepper systems of varying mechanical condition and/or tracking quality.

For the four Target Guide Steppers (Burdette Medical Systems, Inc., Champaign, IL) we have tested, the mean of LRE was 0.32 mm with a standard deviation of 0.18 mm. This was consistent with the results of the previous tests with multiple TRUS scanners using a Target-Guide Stepper (Table IV).

More importantly, we found that Accuseed DS 300 achieved a significantly higher calibration accuracy and precision than Target Guide steppers: the LRE mean of the

TABLE IV. Validation results of iCAL tested with different TRUS scanners.[a]

TRUS Scanner	LRE: mm Mean	LRE: mm Std	Frequency (MHz)	Depth (cm)	Data Interface	Type	Age
Leopard 2001	0.37	0.23	6.5	9.0	S-video	Full	1990s
Sonix MDP 4.0	0.38	0.24	6.0	7.0	S-video	Full	2000s
Sonix TOUCH (analogue)	0.33	0.25	6.0	7.0	S-video	Full	2010s
Sonix TOUCH (digital)	0.37	0.27	6.0	7.0	Ulterius Digital	Full	2010s
Terason 2000	0.35	0.26	Norm	8.0	S-video	Laptop	2000s
VLCUS	0.41	0.26	Norm	7.0	S-video	Portable	1990s
Average	**0.37**	**0.25**	—	—	—	—	—

[a]All tests used the same Target Guide Stepper (Burdette Medical Systems).

Accuseed was one half that of the Target Guides (0.16 mm versus 0.32 mm), with a much smaller standard deviation as well (0.10 mm versus 0.18 mm). This result is due to the fact that the Accuseed DS 300 stepper provides higher position-tracking accuracy than the Target Guide stepper and is also mechanically more stable and precise in design.

Finally, there are two significant clinical implications of these findings. First, any improvement in the stepper tracking accuracy and precision, and the mechanical stability may significantly improve the brachytherapy calibration. Second, iCAL is capable of providing a means of real-time quality assurance of the brachytherapy stepper systems in the operating room, by monitoring and reporting any unexpected change in the calibration accuracy and precision in an intraoperative brachytherapy procedure.

III.E. Results of needle insertion to validate template-TRUS calibration

Table VI shows the TRE results of the template-TRUS calibration accuracy of iCAL. The brachytherapy needles used in the tests are 18-gauge Mick TP Prostate Seeding Needles (Mick Radio-Nuclear Instruments, Inc., Bronx, NY), having a 1.270 ± 0.013 mm outer diameter. The TRUS image has a size of 640×480 pixels and a resolution of 0.2 mm/pixel (or 5 pixels per millimeter).

Our key observations and findings include the following. The TREs were all below 1 mm in the seven needle-insertion experiments, with an average of 0.56 mm and a standard deviation of 0.27 mm. These results suggest an excellent template-TRUS calibration accuracy and precision of iCAL.

Further, the TRE measurements are consistent with the sub-millimeter LRE results reported in Tables III–V.

Finally, the tested locations where the needles were inserted (C3, C5, D5, E3, E5, b4, and e4) encompassed the targeted area of the prostate in a clinical setup. Therefore the TRE measured in this setup provides a good approximation of the template-TRUS calibration accuracy using iCAL in the operating room.

Figure 10 shows a visual confirmation of the results: the template grid (in green) was registered to the TRUS images by iCAL and displayed to the user in real time while the needles were being inserted through the grid holes in the water tank. As can be clearly observed, the needle artifacts in the TRUS image, which were the corresponding positions of the needle tip inserted through grid holes C5, D5, E5, b4, e4, C3, and E3, all perfectly coincided with the template grid positions computed by iCAL, showing excellent TRE.

TABLE V. Validation results of iCAL tested with different brachytherapy steppers.[a]

Brachytherapy Stepper	LRE: mm Mean	LRE: mm Std	Manufacturer
Target guide #1	0.25	0.16	Burdette Medical Systems, Inc., Champaign, IL
Target guide #2	0.34	0.21	
Target guide #3	0.33	0.25	
Target guide #4	0.36	0.10	
Target guide stepper (average)	**0.32**	**0.18**	
Accuseed DS 300	**0.16**	**0.10**	Computerized Medical Systems, Inc., Saint Louis, MO

[a]TRUS images acquired by Sonix TOUCH Analogue (Ultrasonix Corp.).

TABLE VI. TRE results of needle insertion to validate template-TRUS calibration accuracy.

Template grid	C3	C5	D5	E3	E5	b4	e4	**Mean**	**Std**
TRE (mm)	0.31	0.25	0.91	0.56	0.88	0.35	0.69	**0.56**	**0.27**

III.F. Results of 3D overlay of template to TRUS

Figure 11 displays the 3D overlay of the template grids on the real-time TRUS images, after the calibration parameters were computed by iCAL. The green grid matrix in the view is the front, painted face of the template and the rear gray-scale image is the real-time TRUS images (in this particular case showing the N-wires of the iCAL phantom). The user can interact with the 3D display to translate, rotate and zoom in/out the 3D overlay (four arbitrary viewing angles and positions are shown in Fig. 11).

Because the positions of both the TRUS probe and the template are tracked in real-time by the stepper (and monitored by iCAL), iCAL will accurately update and display any position change of the TRUS image and the template grids while the user translates or rotates the TRUS transducer during the scan, or displaces the template back or forth.

IV. DISCUSSION AND CONCLUSIONS

To the best of our knowledge, this is the first automated method proposed for the template calibration of brachytherapy systems, primarily designed and intended to be

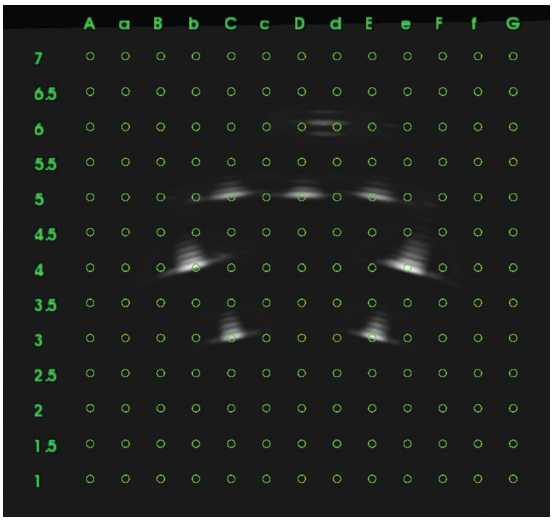

FIG. 10. Needle insertion to validate template-TRUS calibration accuracy (TRE).

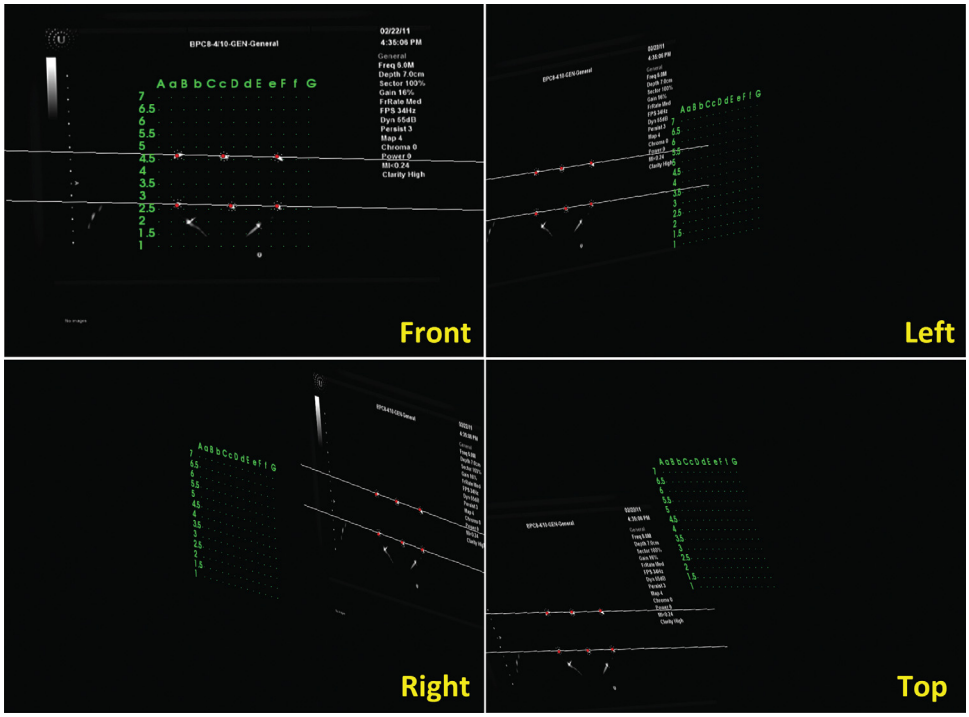

FIG. 11. Results of the final, real-time 3D overlay of the template to TRUS.

performed in the operating room while the patient is being prepared for surgery. The method is fast and solely computation based, to avoid subjectivity and human errors. The elimination of the conventional, lengthy, laborious, and periodic calibration sessions will achieve two main goals simultaneously: it may make the brachytherapy system more accurate and consistent, as well as much less expensive.

In a general sense, the novelty of the proposed iCAL system pertains to ultrasound-guided needle insertion procedures, where surgical end-effectors (such as a template, needle guide, needle holder or robotic needle driver) and TRUS images are spatially coregistered. The basic idea is to mechanically couple a precision-made calibration device with the surgical end-effector. There are many possible ways to do that, however, for manufacturing simplicity and to preempt sterilization issues in the operating room (i.e., the template needs to be sterilized during each treatment, thus making it impractical to directly assemble a calibration device with the template), we took the approach to combine the calibration phantom and an exact exterior replica of the surgical end-effector (template) as one unibody member.

This principle can be equally applied to other forms and flavors of transperineal prostate interventions, including but not limited to localized therapies (thermal ablation, cryo ablation, injections, etc.) and biopsy of the prostate.

We encountered a number of challenges in the design and development of iCAL. First of all, to make for easy access to the inner wires of the iCAL phantom, we incorporated a large opening of the container box (Fig. 4). This created difficulties to seal the water in the phantom. The weight of the water (about 900 grams) built up pressure inside the container box and caused slow water dripping along the edges of the rubber seal. In the final production, the phantom will be sealed with tissue-mimicking gel that is less prone to the problem of leakage. We are also experimenting with optimal designs (e.g., to reduce the weight of the water by downsizing the container) and better sealing methods to make the phantom completely dry.

Another challenge was to have the TRUS probe get in sufficient contact with the rubber window of the iCAL phantom for proper imaging. Naturally, ultrasound gel was used to provide acoustic coupling between the transducer crystals and the rubber window. However, because the iCAL phantom was mounted directly on the brachytherapy template holder on top of the transverse transducer (Fig. 2), due to gravity, the coupling gel easily fell out when the probe was being displaced and rotated underneath the rubber window, causing a loss of visibility of the phantom during imaging. We are exploring more efficient and reliable coupling methods to resolve this issue.

The weight of the phantom has caused one more problem. With the water sealed inside, the complete phantom assembly weights about 1.8 kilograms. Since the entire phantom is affixed on the brachytherapy template holder, the weight caused the phantom to sag down a little, introducing errors into the calibration. This problem has been easily remedied by lifting the sagging end of the phantom using a supporting stand. In the next release, we will optimize the phantom taking weight and size into consideration and provide weight support.

Essentially, all the aforementioned challenges belong to the category of production engineering, where our work is currently underway to make iCAL ready for clinical application.

In this work, iCAL only calibrated the transverse image of the TRUS probe to the brachytherapy template. Our next step is to extend the automated calibration method to the sagittal image plane, so that both the transverse image and the sagittal image produced by the TRUS probe can be accurately coregistered and compounded together to produce more accurate TRUS volume.

Finally, it is important to note that iCAL ascertains the intrinsic quality of a brachytherapy system (i.e., the accuracy of the brachytherapy device itself), but it does not prevent extrinsic errors caused by needle bending/deflection, tissue deformation or organ motion. These errors are contributed by random, unforeseeable factors that typically cannot be detected during the system-calibration stage.

In summary, we proposed a new device and an automatic, computation-based calibration solution for brachytherapy systems, to be used in the operating room while the patient is prepared for surgery. Four types of independent phantom or TRE validation experiments were performed. In all the experiments, the proposed method has consistently achieved sub-millimeter accuracy and precision, as well as a high robustness and compatibility in dealing with different commercial ultrasound machines and brachytherapy steppers. In the 50 independent, real-time calibration trials, an average of 0.57 ± 0.13 mm reconstruction error was achieved relative to the ground truth. The averaged reconstruction error was 0.37 ± 0.25 mm with six different commercial TRUS scanners and 0.29 ± 0.16 mm with five different commercial stepper systems. Finally, the TRE with needle insertions through the template was 0.56 ± 0.27 mm on average relative to the ground truth. These results demonstrate that iCAL is capable of providing an accurate, robust, and efficient means of quality assurance in the operating room.

ACKNOWLEDGMENTS

This research was supported by the Natural Sciences and Engineering Research Council of Canada (NSERC) Idea to Innovation Grant, Acoustic MedSystems, Inc., and Queen's University. Thomas Kuiran Chen was also the recipient of a 2010–2011 MITACS Accelerate Ph.D. Fellowship. Dr. Gabor Fichtinger is Cancer Care Ontario Research Chair.

[1]A. Jemal, F. Bray, M. M. Center, J. Ferlay, E. Ward, and D. Forman, "Global cancer statistics," Ca-Cancer J. Clin. **61**(2), 69–90 (2011).
[2]M. J. Zelefsky, Y. Yamada, G. N. Cohen, A. Shippy, H. Chan, D. Fridman, and M. Zaider, "Five-year outcome of intraoperative conformal permanent i-125 interstitial implantation for patients with clinically localized prostate cancer," Int. J. Radiat. Oncol., Biol., Phys. **67**, 65–70 (2007).
[3]G. S. Merrick, P. D. Grimm, J. Sylvester, J. C. Blasko, W. M. Butler, Z. A. Allen, U.-U.-H. Chaudhry, A. Mazza, and M. Sitter, "Initial analysis of pro-qura: A multi-institutional database of prostate brachytherapy dosimetry," Brachytherapy **6**(1), 9–15 (2007).
[4]J. T. Wei, R. L. Dunn, H. M. Sandler, P. W. McLaughlin, J. E. Montie, M. S. Litwin, L. Nyquist, and M. G. Sanda, "Comprehensive comparison of health-related quality of life after contemporary therapies for localized prostate cancer," J. Clin. Oncol. **20**, 557–566 (2002).
[5]D. C. Miller, M. G. Sanda, R. L. Dunn, J. E. Montie, H. Pimentel, H. M. Sandler, W. P. McLaughlin, and J. T. Wei, "Long-term outcomes among localized prostate cancer survivors: Health-related quality-of-life changes after radical prostatectomy, external radiation, and brachytherapy," J. Clin. Oncol. **23**, 2772–2780 (2005).
[6]M. Zerhouni and M. Rachedine, "Ultrasonic calibration material and method," U.S. patent 5196343 (March 23, 1993).
[7]A. Goldstein, M. Yudelev, R. K. Sharma, and E. Arterbery, "Design of quality assurance for sonographic prostate brachytherapy needle guides," J. Ultrasound Med. **21**, 947–954 (2002).
[8]S. Mutic, D. A. Low, G. H. Nussbaum, J. F. Williamson, and D. Haefner, "A simple technique for alignment of perineal needle template to ultrasound image grid for permanent prostate implants," Med. Phys. **27**, 141–143 (2000).
[9]T. Peters, *Image-Guided Interventions: Technology and Applications*, 1st ed. (Springer, New York, 2008).
[10]C. D. Barry, C. P. Allott, N. W. John, P. M. Mellor, P. A. Arundel, D. S. Thomson, and J. C. Waterton, "Three-dimensional freehand ultrasound: Image reconstruction and volume analysis," Ultrasound Med. Biol. **23**(8), 1209–1224 (1997).
[11]R. W. Prager, R. N. Rohling, A. H. Gee, and L. Berman, "Rapid calibration for 3D freehand ultrasound," Ultrasound Med. Biol. **24**, 855–869 (1998).
[12]D. M. Muratore and R. L. Galloway Jr., "Beam calibration without a phantom for creating a 3D freehand ultrasound system," Ultrasound Med. Biol. **27**(11), 1557–1566 (2001).
[13]E. M. Boctor, A. Jain, M. A. Choti, R. H. Taylor, and G. Fichtinger, "Rapid calibration method for registration and 3D tracking of ultrasound images using spatial localizer," *Proceedings of SPIE Medical Imaging: Ultrasonic Imaging and Signal Processing*, edited by W. F. Walker and M. F. Insana (SPIE, San Diego, CA, 2003), Vol. 5035, pp. 521–532.
[14]N. Pagoulatos, D. R. Haynor, and Y. Kim, "A fast calibration method for 3D tracking of ultrasound images using a spatial localizer," Ultrasound Med. Biol. **27**(9), 1219–1229 (2001).
[15]F. Lindseth, G. A. Tangen, T. Langø, and J. Bang, "Probe calibration for freehand 3D ultrasound," Ultrasound Med. Biol. **29**(11), 1607–1623 (2003).
[16]W. Y. Zhang, R. N. Rohling, and D. K. Pai, "Surface extraction with a three-dimensional freehand ultrasound system," Ultrasound Med. Biol. **30**(11), 1461–1473 (2004).
[17]T. K. Chen, "A system for ultrasound-guided computer-assisted orthopaedic surgery," Master's thesis, Queen's University, Kingston, Ontario, Canada, 2005.
[18]P.-W. Hsu, R. W. Prager, A. H. Gee, and G. M. Treece, "Real-time freehand 3D ultrasound calibration," *Proceedings of SPIE Medical Imaging: Ultrasonic Imaging and Signal Processing*, edited by S. Y. Emelianov and S. A. McAleavey (San Diego, CA, 2007), Vol. 6513, pp. 6513081–6513088.
[19]T. K. Chen, A. D. Thurston, M. H. Moghari, R. E. Ellis, and P. Abolmaesumi, "A real-time ultrasound calibration system with automatic accuracy control and incorporation of ultrasound section thickness," *SPIE Medical Imaging 2008: Visualization, Image-guided Procedures, and Modeling*, edited by M. I. Miga and K. R. Cleary (SPIE, San Diego, CA, 2008), Vol. 6918, pp. 69182A, Best Student Paper Award—Second Place and Cum Laude Poster Award.
[20]E. M. Boctor, I. Iordachita, M. A. Choti, G. Hager, and G. Fichtinger, "Bootstrapped ultrasound calibration," Stud. Health Technol. Inform. **119**, 61–66 (2006).
[21]D. C. Barratt, G. P. Penney, C. S. K. Chan, M. Slomczykowski, T. J. Carter, P. J. Edwards, and D. J. Hawkes, "Self-calibrating 3D-ultrasound-based bone registration for minimally invasive orthopedic surgery," IEEE Trans. Med. Imaging **25**(3), 312–323 (2006).
[22]E. M. Boctor, I. Iordachita, G. Fichtinger, and G. D. Hager, "Ultrasound self-calibration," *Proceedings of SPIE Medical Imaging: Visualization, Image-Guided Procedures, and Display*, edited by K. R. Cleary and R. L. Galloway, Jr. (SPIE, San Diego, CA, 2006), Vol. 6141, pp. 61412N1–61412N12.
[23]L. Mercier, T. Langø, F. Lindseth, and L. D. Collins, "A review of calibration techniques for freehand 3-D ultrasound systems," Ultrasound Med. Biol. **31**(4), 449–471 (2005).
[24]A. Ng, A. Beiki-Ardakan, S. Tong, D. Moseley, J. Siewerdsen, D. Jaffray, and I. W. T. Yeung, "A dual modality phantom for cone beam CT and ultrasound image fusion in prostate implant," Med. Phys. **35**, 2062–2071 (2008).
[25]G. Booch, I. Jacobson, and J. Rumbaugh, *Unified Modeling Language User Guide (Object Technology)* (The Addison-Wesley Object Technology Series, Addison-Wesley Professional, 1998).
[26]D. W. Eggert, A. Lorusso, and R. B. Fisher, "Estimating 3D rigid body transformations: A comparison of four major algorithms," Mach. Vision Appl. **9**(5–6), 272–290 (1997).

[27]E. M. Boctor, I. Iordachita, G. Fichtinger, and G. D. Hager, "Real-time quality control of tracked ultrasound," Lect. Notes Comput. Sci. **3749**, 621–630 (2005).
[28]W. R. Hedrick, D. L. Hykes, and D. E. Starchman, *Ultrasound Physics and Instrumentation*, 4th ed. (Elsevier Mosby, Missouri, 2005).
[29]S. Meairs, J. Beyer, and M. Hennerici, "Reconstruction and visualization of irregularly sampled three- and four-dimensional ultrasound data for cerebrovascular applications," Ultrasound Med. Biol. **26**, 263–272 (2000).
[30]R. W. Prager, A. Gee, and L. Berman, "Stradx: Real-time acquisition and visualization of freehand three-dimensional ultrasound," Med Image Anal. **3**, 129–140 (1999).
[31]D. G. Gobbi, "Brain deformation correction using interactive 3D ultrasound imaging," Ph.D. thesis, University of Western Ontario, London, ON, Canada, 2003.
[32]M. J. Gooding, S. H. Kennedy, and J. A. Noble, "Temporal calibration of freehand three-dimensional ultrasound using image alignment," Ultrasound Med. Biol. **31**, 919–927 (2005).
[33]M. Nakamoto, Y. Sato, K. Nakada, Y. Nakajima, K. Konishi, M. Hashizume, and S. Tamura, "A temporal calibration method for freehand 3D ultrasound system: A preliminary result," CARS, p. 1365 (2003).
[34]F. Rousseau, P. Hellier, and C. Barillot, "A novel temporal calibration method for 3D ultrasound," IEEE Trans. Med. Imaging **25**(8), 1108–1112 (2006).
[35]G. M. Treece, A. H. Gee, R. W. Prager, C. J. C. Cash, and L. H. Berman, "High-definition freehand 3-d ultrasound," Ultrasound Med. Biol. **29**, 529–546 (2003).
[36]T. K. Chen, A. D. Thurston, R. E. Ellis, and P. Abolmaesumi, "A real-time freehand ultrasound calibration system with automatic accuracy feedback and control," Ultrasound Med. Biol. **35**(1), 79–93 (2009).
[37]L. Sciavicco and B. Siciliano, *Modelling and Control of Robot Manipulators*, 2nd ed. (Springer, New York, 2000).
[38]J. W. Trobaugh, D. J. Trobaugh, and W. D. Richard, "Three-dimensional imaging with stereotactic ultrasonography," Comput. Med. Imaging Graph. **18**(5), 315–323 (1994).
[39]F. Lindseth, J. Bang, and T. Lang, "A robust and automatic method for evaluating accuracy in 3D ultrasound-based navigation," Ultrasound Med. Biol. **29**, 1439–1452 (2003).
[40]P.-W. Hsu, R. W. Prager, A. H. Gee, and G. M. Treece, "Real-time freehand 3D ultrasound calibration," Ultrasound Med. Biol. **34**, 239–251 (2008).